AJNR

Adaptive changes of autoregulation in chronic cerebral hypotension with arteriovenous malformations: an acetazolamide-enhanced single-photon emission CT study.

L Hacein-Bey, R Nour, J Pile-Spellman, R Van Heertum, P D Esser and W L Young

Adaptive Changes of Autoregulation in Chronic Cerebral Hypotension with Arteriovenous Malformations: An Acetazolamide-Enhanced Single-Photon Emission CT Study

Lotfi Hacein-Bey, Ramy Nour, John Pile-Spellman, Ronald Van Heertum, Peter D. Esser, and William L. Young

PURPOSE: To evaluate the relationship among feeding arterial pressure, lesion size, and perfusion in cerebral cortex adjacent to cerebral arteriovenous malformations (AVMs). **METHODS:** Eleven patients with hemispheric AVMs underwent ^{99m}Tc hexamethyl-propyleneamine oxime single-photon emission CT before and after 1 g of acetazolamide was administered intravenously. AVM volume was estimated from MR dimensions and measured according to the method described by Pasqualin. Pressure measurements were obtained in arteries feeding the cortex adjacent to AVMs. Single-photon emission CT regions of interest were defined in cortex adjacent to the AVM and compared with contralateral regions using the Mountz method to estimate a baseline and dynamic (acetazolamide-challenged) perfusion defect volume. **RESULTS:** Eight of 11 patients had baseline perfusion defects, but these defects were unrelated to feeding artery pressures ($y = -.06x + 9.92$, $r^2 = .04$) or the dynamic change in defect volume after acetazolamide administration ($y = .01x + .02$, $r^2 = .002$). However, there was a correlation between AVM volume and the baseline defect volume ($y = .75x - 1.9$, $r^2 = .76$). Five patients had increased defect volume after acetazolamide administration; 5 patients had either no change in or improvement of perfusion. Dynamic changes in defect volume were related to feeding artery pressures. **CONCLUSION:** Perilesional baseline perfusion defects appear to be related to lesion size and not to local arterial pressure. Cerebrovascular reserve generally was preserved, and perfusion defects appeared to be more pronounced with lower arterial pressures in feeding vessels. Although vasodilatory testing can unmask hemodynamic failure with severe local hypotension, baseline perfusion defects near the lesion and distant perfusion changes are more likely attributable to other causes such as mass-related or neurogenic changes.

Index terms: Arteriovenous malformations, cerebral; Brain, pressure; Single-photon emission computed tomography

Cerebral arteriovenous malformations (AVMs) may affect neighboring cerebral tissue by mass effect from edema, venous varix (1), seizure activity (2) or metabolic depression

similar to diachisis (3). However, it is commonly thought that perfusion changes in patients with AVMs are the result of a loss of autoregulation and hemodynamic failure (4, 5). The presumption of pretreatment cerebral "steal" and posttreatment "normal perfusion pressure breakthrough" presupposes the lower limit of autoregulation to be approximately 50 mm Hg and that chronic hypotension results in "vasomotor paralysis" (4, 6). We have previously described autoregulatory vasoconstriction to be intact with arterial pressures as low as 30 mm Hg and have proposed that an adaptive displacement of autoregulatory capacity occurs in hypotensive vascular beds adjacent to the AVM (7).

In this study, we focused on the lower end of the cerebrovascular autoregulatory curve by studying cortical perfusion changes around AVMs with acetazolamide-enhanced single-photon emission computed tomography (CT). Acetazolamide is a potent carbonic anhydrase inhibitor that results in cerebrovascular vasodilation and its administration has been described as a method to demonstrate decreased or absent cerebrovascular reserve (8, 9).

Materials and Methods

Patients and Overview of Study

Eleven patients with supratentorial AVMs (6 women, 5 men) 18 to 59 years of age (mean, 35 years) were referred to us for treatment, which would consist of staged transarterial embolization followed by either surgery or radiosurgery. All patients gave informed consent to participate in a study within the Columbia University AVM Project that would explore cerebral vasoregulation. The initial phase of the study was to obtain a pretreatment ^{99m}Tc hexamethyl-propyleneamine oxime (HMPAO) single-photon emission CT study before and after acetazolamide challenge. The next phase consisted of obtaining intraarterial pressure measurements during sequential embolization sessions. Embolization procedures began within several weeks of the initial evaluation and were separated by a few weeks. In a subgroup of 9 patients, studies were performed to test autoregulatory vasoconstriction in a main pedicle that fed both AVM and normal adjacent cortex. Data from this previously published study (10) are compared with those of the present study.

All patients underwent ^{99m}Tc HMPAO single-photon emission CT before and after the intravenous injection of 1 g of acetazolamide. Images were acquired on a rotating triple-head single-photon emission CT gamma camera (Prism, Picker, Cleveland, Ohio) with resolution of 7.8 mm using low-energy, ultrahigh-resolution fan beam collimation. Acquisition consisted of a multiple rapid acquisition sequence technique. Radius of rotation was less than 14 cm. Each rotation involved continuous motion acquisition for 300 seconds, with each head rotating 120°. The acquisition matrix size was 128 by 128. Four to six rotations were performed for each scan, and each individual rapid acquisition sequence was examined for movement before summation and reconstruction. A low-dose–high-dose (split-dose) protocol was used.

The initial scan was done with an injected dose range of 314 to 396 MBq (8.5 to 10.7 mCi) and the second scan with an injected dose range of 685 to 766 MBq (18.5 to 20.7 mCi). Acquisition began 30 minutes after tracer injection. Thirty minutes after the commencement of the baseline acquisition, 1 g of intravenous acetazolamide was injected. Another 30 minutes were observed before injecting the second dose of tracer, and again the second acquisition was started after 30 minutes. No method for confirming the intravascular administration of acetazolamide was used.

After ramp filter back-projection and attenuation correction, a three-dimensional Butterworth filter (order, 5; cut-off, 0.31 to 0.35) was applied during reconstruction. Transaxial images were oriented to the canthomeatal plane. Each pair of patient studies (baseline/acetazolamide) was manually coregistered (Neuro 900, Strichman Medical, Medfield, Mass) and the low-dose study (corrected for radioisotope decay) was subtracted from the high-dose acquisition to produce a true (net) high-dose scan (DIP Station software HIPG, Hayden Imaging Processing Group, Boulder, Colo). Normalization of the counts measured in each study was made to the true injected dose (preinjection activity minus residual syringe activity) decayed to time of scan commencement.

AVM Volume and Regions of Interest

AVM dimensions were determined from anatomic studies (CT, magnetic resonance, angiograms) and operator transferred (L.H.-B.) onto a standard brain atlas template (Eastman Kodak, Rochester, NY) in the axial, coronal, and sagittal planes. AVM volume was estimated as described by Pasqualin et al (11) and also was rated as small ($<$10 cm^3), medium (between 10 and 20 cm^3), or large ($>$20 cm^3). The AVM contour was carefully drawn with respect to its relationship to surrounding anatomic structures. Then, the AVM nidus was mapped onto the baseline single-photon emission CT axial images using the previously drawn brain atlas images. Both the brain atlas template and the single-photon emission CT studies were obtained 15° above the canthomeatal line. Care was taken not to include adjacent cortical structures in the AVM region of interest and to ensure the exclusion of the AVM defect from the cortical region of interest analysis.

Cortical regions of interest were drawn on the baseline single-photon emission CT studies (Fig 1); standard region of interest width was 6 pixels (13.2 mm). For peri-AVM cortex evaluation, the regions of interest were drawn at the AVM nidus level (see Figs 6 through 8), and encompassed two sections on the single-photon emission CT studies in the axial plane. The cortical region of interest was selected in the same arterial territory as the AVM and distal to its nidus.

Counts were obtained for each cortical region of interest on the AVM side and for the mirrored symmetric contralateral cortical region of interest, thus allowing evaluation of "effective volumes of cerebral tissue" as described by Mountz (12). The original technique, proposed for hemispheric comparisons, was modified to consider a smaller cortical region of interest. The Mountz method expresses partial count loss into a single volume of absolute loss of perfusion. A variation of two SDs from the mean counts was accepted as being within normal limits, and a statistical defect (V_{stat}) was measured as follows:

$$V_{stat} = \frac{mean - 2\,SD}{mean} \times (\text{\# pixels}) \times (\text{pixel volume}).$$
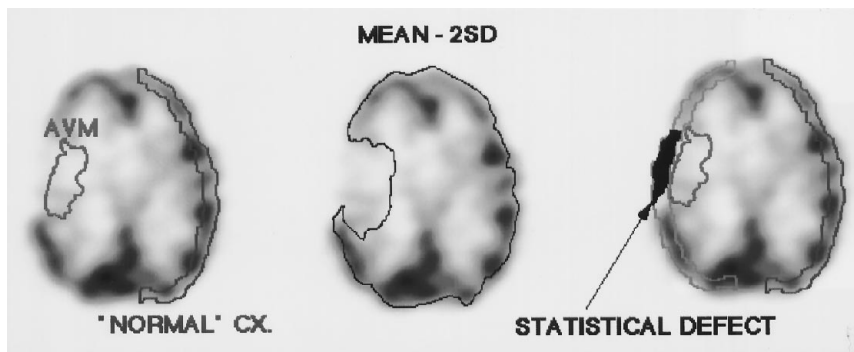
Fig 1. Determination of the cortical defect near the AVM using the *z* score method. Once a defect was detected in a cortical region of interest, statistical analysis was performed to determine whether the defect was significant. Then the effective volume loss is calculated. This analysis is repeated for the postacetazolamide study to determine the "dynamic defect." See text for explanations.

The volume loss (V_{defect}) is assessed by comparing the ipsilateral counts in the cortical region of interest (C_{ipsi}) relative to the contralateral normal side (C_{contra}), as shown in the following equation:

$$V_{defect} = \frac{C_{contra} - C_{ipsi}}{C_{contra}} \times (\# \text{ pixels}) \times (\text{pixel volume}).$$

The V_{defect} was determined for the baseline study (baseline perfusion defect) and after acetazolamide administration. Figure 1 shows how the defect is determined in the easy case of a right subcortical AVM selected for the sake of demonstration; a *z* score analysis is used to map out cortical regions with a count activity within two SDs of the mean.

A dynamic perfusion defect was calculated by subtracting postacetazolamide defect from baseline defects.

Pressure Measurements

Pressure measurements in the artery supplying the cerebral territory adjacent to the AVM were obtained in all patients during embolization procedures done under neurolept intravenous sedation (13). Although distal AVM feeding artery pressures also were measured, the pressure values referred to in this study pertain to arteries feeding normal cortex adjacent to AVMs. Normal cortex was defined as showing a capillary blush without evidence of arteriovenous shunting and being at least one gyrus away from the apparent AVM margin. Pressures were measured as previously described (14, 15). A 1.5F microcatheter (Magic, Balt, Montmorency, France) was advanced into the cortical artery, usually at the M3-4 or M4-5 division level under fluoroscopic guidance. A strain gauge (Transpac, Abbott Critical Care, North Chicago, Ill) transduced the proximal catheter port. Distal pressure was compared with simultaneously obtained systemic arterial pressure (see Table 2) measured in the cervical access artery (internal carotid or vertebral artery) from the introducer catheter.

Data Analysis

Linear regression or analysis of variance was used for parametric data or χ^2 analysis for nonparametric data. The correlation between dynamic perfusion defect volume and feeding artery pressure also was tested with Spearman rank correlation. Results are given as mean $\pm$ SD.

Results

Clinical data are shown in Table 1. AVM locations were frontal (n = 5), temporal (n = 3), parietal (n = 1), occipital (n = 1), and deep choroidal (n = 1). Two AVMs were large, three

TABLE 1: Clinical data: 11 cerebral arteriovenous malformations

Patient	Age, y	Sex	Size	Location	Extension	Presentation
A	24	M	Small	Temporal	Cortical	Seizure*
B	38	M	Small	Occipital	Cortical	Seizure
C	18	F	Large	Parietal	Cortical	Hemorrhage
D	32	F	Large	Frontal	Cortical	Seizure
E	33	F	Small	Frontal	Cortical	Seizure
F	48	F	Small	Basal ganglia	Subcortical	Hemorrhage
G	27	M	Small	Frontal	Cortical	Hemorrhage†
H	20	M	Small	Frontal	Mixed	Seizure
I	59	M	Medium	Temporal	Subcortical	Hemorrhage
J	49	F	Medium	Temporal	Cortical	Hemorrhage
K	34	F	Medium	Frontal	Cortical	Seizure, deficit

* Patient had previous radiosurgery.
† Patient had coexisting moyamoya-type middle cerebral artery stem occlusion.

TABLE 2: Physiologic data: 11 cerebral arteriovenous malformations

Patient	Arterial Pedicle	Feeding Arterial Pressure, mm Hg	Systemic Arterial Pressure, mm Hg	Cortical Perfusion around AVM*	
				Baseline Perfusion Defect	Dynamic Perfusion Defect
A	M3	29	63	No defect	Worse
B	A2	69	84	No defect	Improved
C	M3	38	67	Defect	No change
D	M2	29	81	Defect	Worse
E	M2	42	63	Defect	No change
F	M1	53	54	Defect	No change
G	Lenticulostriate	31	109	Defect	Worse
H	M2	83	95	No defect	Worse
I	P2	81	88	Defect	No change
J	M2	59	80	Defect	Improved
K	M3	33	60	Defect	Not available

* Cortical perfusion around arteriovenous malformation (AVM) refers to the following: On baseline single-photon emission CT studies peri-AVM cortical perfusion is represented as the presence or absence of a defect relative to contralateral cortical perfusion (baseline perfusion defect). After acetazolamide challenge, peri-AVM cortical perfusion was assessed as net defect volume using a modified Mountz method (dynamic perfusion defect).

were medium, and six were small. Eight AVMs were predominantly cortical, two were subcortical, and one was mixed. Clinical presentation was with seizures in five patients and with hemorrhage in five, and one patient had both seizures and a transient hemiparesis. One patient with a small right temporal AVM and seizures had received radiation treatment 3 years before this study. One patient with a small right frontal AVM had concomitant moyamoya disease. One patient with a baseline perfusion defect demonstrated no measurable response to acetazolamide at any site in the cerebral hemispheres or the cerebellum and is therefore excluded from subsequent analysis (patient K); in this patient the acetazolamide injection was thought to have been extravascular. There was no effect of AVM location or clinical presentation on feeding artery pressure using analysis of variance (ANOVA).

AVM Size and Feeding Artery Pressure

Physiologic data are shown in Table 2. A weak inverse relationship ($y = -.16x + 19.63$, $r^2 = .19$, $P = .2152$) was found between AVM size and feeding artery pressures, in agreement with previous larger series (16, 17).
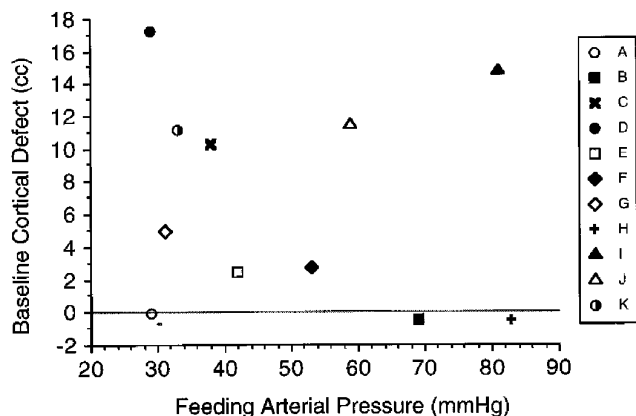
Cortical Perfusion

Eight patients had baseline perfusion defects around the AVM, and three did not. There was no correlation between baseline perfusion de-

fects in the cortex adjacent to the AVM and feeding artery pressures ($y = -.06x + 9.92$, $r^2 = .04$, $P = .6210$) (Fig 2). The baseline perfusion defect volume also was unrelated to the dynamic perfusion defect volume after acetazolamide administration ($y = .01x + .02$, $r^2 = .002$, $P = .8877$). However, there was a strong correlation between AVM size and the size of the baseline perfusion defect ($y = .75x - 1.9$, $r^2 = .76$, $P = .0004$) (Fig 3).
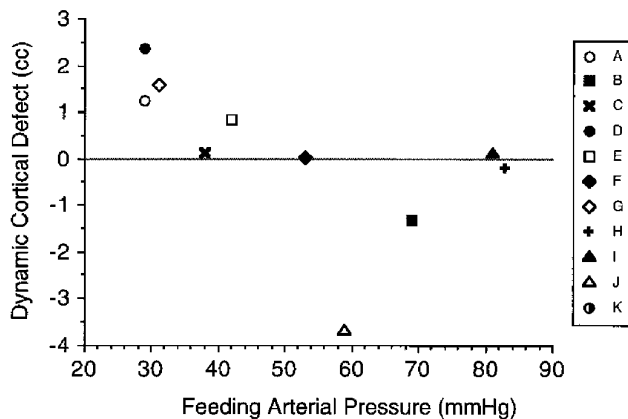
One of the three patients without a baseline perfusion defect around the AVM had a large dynamic perfusion defect after acetazolamide administration. This patient had a low feeding artery pressure (29 mm Hg).

Figure 4 shows the correlation of peri-AVM dynamic perfusion defects as a function of feeding artery pressures ($P = .0145$, Spearman rank correlation). Five patients had various degrees of worsening of cortical perfusion around the AVM after acetazolamide administration, whereas all the other patients had either no changes or improvement of perfusion. The three patients with the lowest feeding artery pressure had the largest change in dynamic perfusion defects after acetazolamide administration.

Change in blood flow with phenylephrine administration from a previous study (10) was compared with baseline cortical perfusion and the postacetazolamide cortical perfusion; there was no relationship. The only patient (patient A) with pressure-passive flow (ie, an increase in cerebral blood flow after phenylephrine admin-
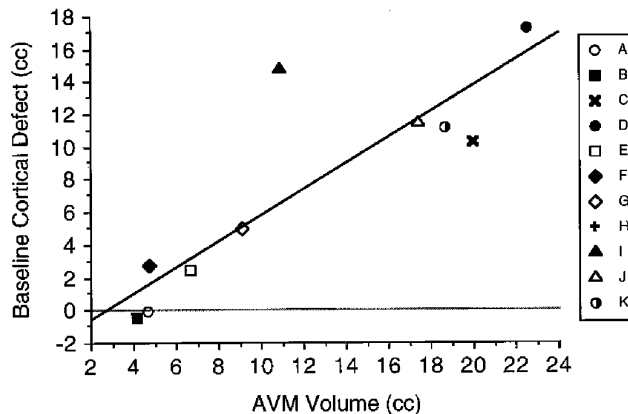
2

3

4

Fig 2. Baseline perfusion defect volume (peri-AVM cortical defect) at baseline versus feeding artery pressure ($y = -.06x + 9.92$, $r^2 = .04$, $P = .6210$).

Fig 3. Baseline perfusion defect volume (peri-AVM cortical defect) versus AVM volume ($y = .75x - 1.9$, $r^2 = .76$, $P = .0004$).

Fig 4. Dynamic perfusion defect after acetazolamide versus feeding arterial pressure. The three patients with the lowest feeding artery pressures had the largest increase in defect volume. The patients with the lowest feeding artery pressure had the largest increase in defect volume after acetazolamide ($P = .0145$, Spearman rank correlation).

istration; see Fig 5) also had a dynamic defect (see Fig 8).

Subcortical Perfusion

Visual assessment was performed using a 10-step color map. Diaschisis, as manifested by a modest decrease in radiotracer activity, was seen in ipsilateral thalamus (n = 8) and contralateral cerebellum (n = 5). Thalamic and cerebellar counts tended to normalize after acetazolamide administration, but the responses were variable and not correlated with feeding artery pressures.

Discussion

AVMs may exert a deleterious effect on brain function by several mechanisms, including mass effects (eg, hematoma, edema, or gradually expanding, abnormal vascular structures such as venous aneurysms), metabolic depression (diaschisis), and seizure activity.

This study is a comparison of distal cerebral arterial pressure measurements in the peri-lesional area of AVMs with a test of cerebrovascular reserve capacity (acetazolamide). There are two primary findings. First, baseline perfusion defects do not correlate with feeding arterial pressures. Second, although perfusion deficits can appear after vasodilation after CO_2 challenge as obtained from acetazolamide administration, it appears to occur at a much lower pressure than is commonly felt to be the lower limit of autoregulation. This "lower limit" corresponds to the left-sided genu of the autoregulation curve (Fig 5), and its normal value has been widely thought to be around 50 to 60 mm Hg (18).

We would interpret our findings to suggest three types of changes induced by AVMs: (a) hemodynamic; (b) neurogenic; and (c) artifactual or mass related.
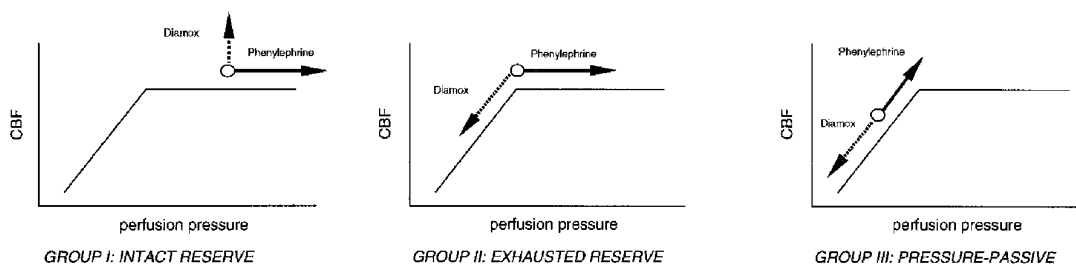
Fig 5. Conceptual representation of possible perfusion patterns in cortex adjacent to AVMs. Patients in group I both have intact cerebrovascular reserve (as assessed by acetazolamide [*Diamox*] challenge) and retain the capability of autoregulatory vasoconstriction to maintain cerebral blood flow (*CBF*) constant with an increase in perfusion pressure. Group II patients are characterized by an exhausted reserve. Under normal circumstances, cerebral blood flow is adequately maintained, despite a low cerebral arterial pressure. Increasing perfusion pressure (eg, with phenylephrine) results in appropriate vasoconstriction to maintain a constant cerebral blood flow. However, acetazolamide-induced vasodilation in adjacent normal regions exceeds the local capacity to vasodilate further, and a dynamic perfusion defect is observed. Group III would include patients that neither dilate nor constrict and represent true "vasoparalysis."

Hemodynamic Changes and the Concept of Failed Autoregulation

A conceptually attractive but unproved paradigm prevails to explain many instances of pretreatment defects—cerebral "steal"—and certain catastrophic posttreatment complications of brain swelling and intracranial hemorrhage. This has been termed *normal perfusion pressure breakthrough* (4) or *circulatory breakthrough* (19). These models propose that: (*a*) perfusion pressure is reduced to the lower limit of autoregulation by both arterial hypotension and venous hypertension in neighboring vascular territories; (*b*) arteriolar resistance in these adjacent territories is at or near a state of maximal vasodilation (if perfusion pressure decreases, steal ensues); (*c*) chronic hypotension results in vasomotor paralysis and deranged autoregulatory capability (6, 20); and (*d*) reversal of arterial hypotension after treatment (6, 21–23) is not matched by a corresponding increase in cerebrovascular resistance and results in hyperemia and, in its worst case, swelling or intracranial hemorrahage (21, 23–28).

Such a model implies that it is not the AVM itself, but rather decreased perfusion pressure in adjacent, functional tissue, that is responsible for both pretreatment ischemic and posttreatment hyperemic symptoms. In principle, this model assumes mechanisms encountered in other conditions of reduced perfusion pressure (eg, occlusive atherosclerotic disease) (18).

However, there is accumulating evidence that adaptive mechanisms allow cerebral blood flow to remain constant after perfusion is increased in cerebral tissue adjacent to AVMs both before (7) and after (10) surgery. Furthermore, the lower limit of autoregulation appears to be shifted to the left (8). This adaptive shift to the left places the lower limit at a level considerably lower than 50 or 60 mm Hg (4, 6) and the presence of chronic hypotension does not necessarily result in vasoparalysis in the arteriolar resistance bed. Although CO_2 reactivity may be impaired in brain regions surrounding AVMs (21), there generally is a preserved responsiveness to CO_2 presurgical and postsurgical resection (29), which lends further support to the notion of intact autoregulatory capacity.

This study explored the lower end of the autoregulatory curve in AVM patients using intraarterial pressure measurements and tomographic imaging (Figs 6 through 8). Our findings indicate that, in general, the capability to vasodilate is preserved in cortical regions adjacent to AVMs, but may be exhausted in some cases. Five of 8 patients with reduced baseline cerebral blood flow near the AVM showed unaltered or improved perfusion after acetazolamide administration (Fig 6 A through D). Only the patients with very low feeding artery pressures (ie, ≈30 mm Hg) experienced a significant cerebral blood flow decrease in the cortex surrounding the AVM (Fig 7). Moreover, one patient (patient A) with normal cerebral blood flow at rest, apparent pressure-passive flow to phenylephrine challenge, and low feeding artery pressure showed a dynamic perfusion defect after vasodilatory stimulus (Fig 8).
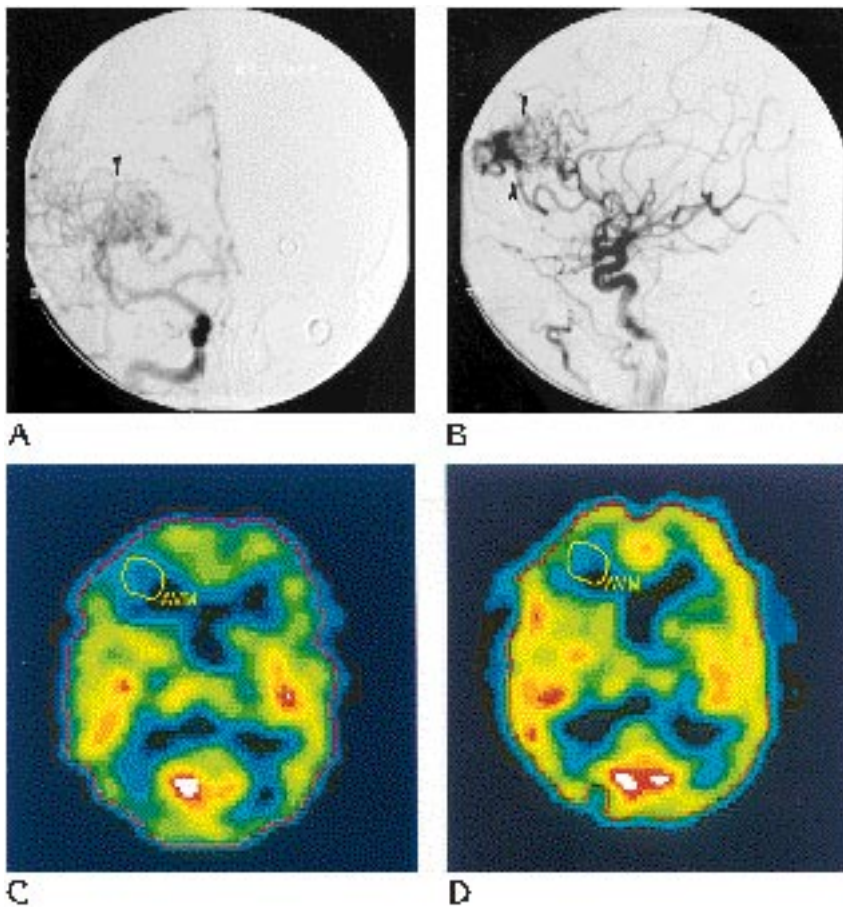
Fig 6. Patient H, example of intact cerebrovascular reserve (group I).

A, Anteroposterior view of a right internal carotid angiogram showing a small right frontal AVM (*arrowheads*).

B, Lateral view of a right internal carotid angiogram showing a small right frontal AVM (*arrowhead*).

C, Axial single-photon emission CT scan at the level of the AVM nidus. Z score analysis reveals that all cortical regions of interest are within normal values (see text); no baseline perfusion defect is present.

D, No dynamic perfusion defect is seen after acetazolamide. Feeding artery pressure was 83 mm Hg.

Comparison with Previously Published Pressure Autoregulation Data

A subgroup of nine patients in this study also underwent testing of autoregulatory vasoconstriction in a main pedicle that fed both AVM and normal adjacent cortex. Data from this previously published study (10) are compared with the results of the present study. Briefly, a bolus of ^{133}Xe was given through the microcatheter and washout recorded from the scalp using a scintillation detector. Systemic arterial pressure was increased ≈ 25 mm Hg by phenylephrine infusion. A second bolus of ^{133}Xe was given, and washout recorded. After exclusion of the shunt spike, initial slope was calculated. Percent change in cerebral blood flow per millimeter of mercury change in cerebral arterial pressure after phenylephrine challenge was calculated (10).

Synthesis of Autoregulation Studies

Combining the acetazolamide single-photon emission CT data and the superselective ^{133}Xe cerebral blood flow measurements with phenylephrine challenge, we can synthesize the general relationships as shown in Figure 5. Patients in group I both have intact cerebrovascular reserve (as assessed by acetazolamide challenge) and retain the capability for autoregulatory vasoconstriction to maintain cerebral blood flow constant with an increase in perfusion pressure; most (60%) of our patients fit into this category (Fig 6).

Group II patients are characterized by an exhausted reserve. Under normal circumstances, cerebral blood flow is adequately maintained, despite a low cerebral arterial pressure. Increasing perfusion pressure (eg, with phenylephrine) results in appropriate vasoconstriction to maintain a constant cerebral blood flow. However acetazolamide-induced vasodilation in adjacent normal regions exceeds the local capacity to vasodilate further, and a dynamic perfusion defect is observed (Fig 7).

Group III would include patients that can neither dilate nor constrict and represent true "vasoparalysis." Only one of our patients displayed

Fig 7. Patient D, example of "exhausted reserve" (group II).

A, Axial contrast-enhanced CT scan showing large right frontal AVM (*arrowheads*).

B, Lateral right internal carotid angiogram showing a large frontal AVM (*arrowheads*) with high-flow shunts.

C, Axial single-photon emission CT study at the level of the AVM nidus. *Z* score analysis reveals a baseline cortical defect at the AVM level (*arrows*).

D, The perfusion defect worsens (*arrows*) after acetazolamide administration. This patient had a low feeding artery pressure (29 mm Hg).
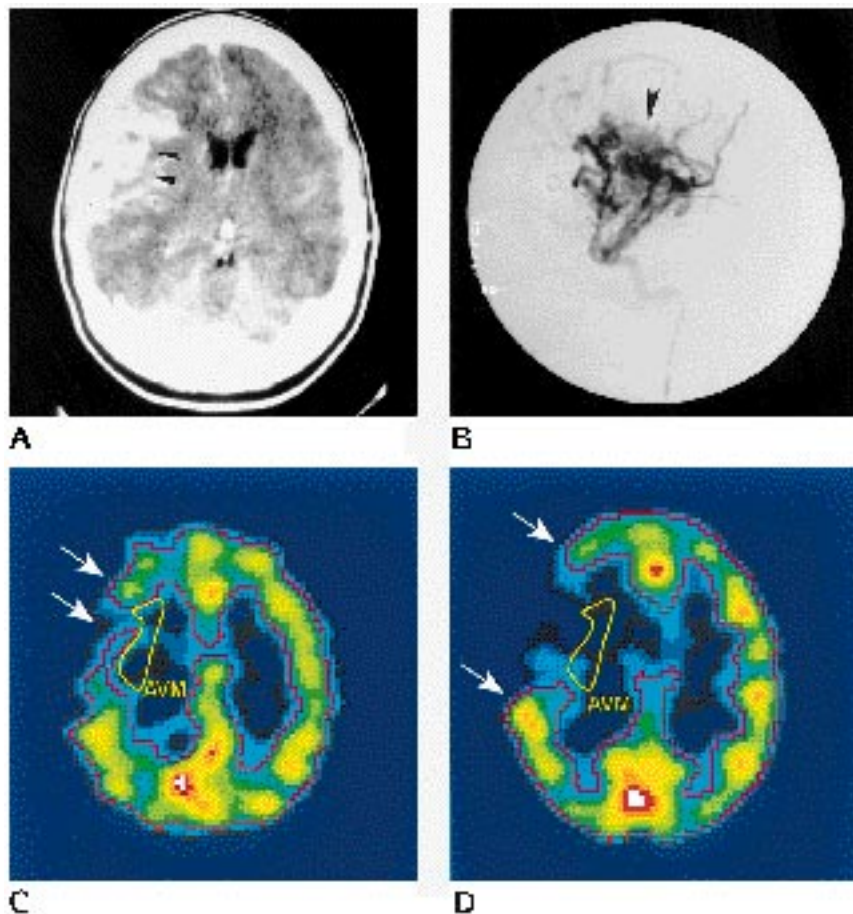
this type of behavior. The observations in this patient may reflect changes induced by a full course of radiosurgery (45 Gy) 3 years previously, with no angiographic evidence of nidus obliteration. Radiation therapy is known to induce subendothelial edema, fibrinoid necrosis, and intimal fibrosis in capillaries, arterioles, and small arteries (30, 31). We believe that prior radiation damage to the peri-AVM vasculature was a likely cofactor in the perfusion pattern observed in this patient with a small temporal AVM and angiomatous changes around the lesion (Fig 8).

Neurogenic Changes in Perfusion

Diaschisis refers to functional alterations in cerebral tissue remote from a lesion (2, 3). This phenomenon, which has best been studied in ischemic stroke, still is poorly understood. Diaschitic brain regions after ischemic injury appear to have preserved CO_2 responsiveness (32). Our qualitative observations of distant subcortical changes confirm other reports that have described diaschisis in thalamus and cerebellum of patients with AVMs (33, 34). It may be that many decreases in cerebral blood flow (35) and cerebral metabolism (36) ascribed to hemodynamic mechanisms (ie, steal) in fact represent diaschisis (37).

Artifactual or Mass-Related Perfusion Changes

Local hypoperfusion immediately adjacent to the nidus has been widely described with single-photon emission CT imaging (38). As important evidence against a simple hemodynamic mechanism for the baseline perfusion defects, Figure 3 suggests that AVM size, rather than feeding arterial pressure, correlates with the volume of the baseline perfusion defect. This is evidence that the apparent "steal" region noted on baseline scans is not related to a territorial reduction in local perfusion pressure. Possible considerations might be imaging artifact (partial volume effects), mass effects of the nidus or associated
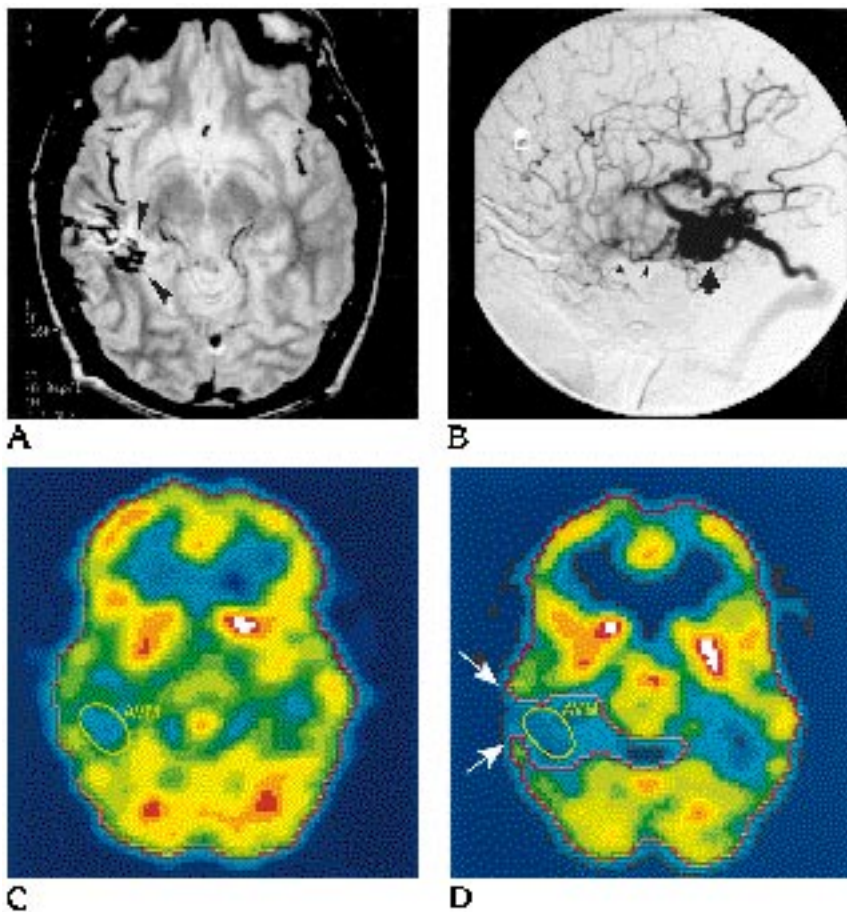
Fig 8. Patient A, example of "vasoparalysis" (group III).

A, Axial T2-weighted magnetic resonance image showing a small right temporal AVM (*arrowheads*) and associated signal changes attributed to radiation changes.

B, Lateral right carotid angiogram showing temporal AVM (*arrow*) with a suggestion of angiomatous changes around AVM (*arrowheads*).

C, Axial single-photon emission CT scan at the level of the AVM; no significant perfusion defect is noted in the cortex adjacent to the AVM.

D, Postacetazolamide axial single-photon emission CT scan; a cortical perfusion defect is measured (*arrows*). This patient had a low feeding artery pressure (29 mm Hg). At baseline, perfusion is adequate; vasodilation results in suboptimal cerebral blood flow. Of note, this patient also had a phenylephrine challenge and responded to it by increasing cerebral blood flow in the cortex around the AVM; vasoconstriction also was impaired.

vascular structures such as venous aneurysms (1, 39), or possibly isolated venous hypertension (40, 41). Furthermore, baseline perfusion defect was not related to change in defect volume with acetazolamide. If the baseline perfusion defect was attributable solely to hemodynamic causes, physiologic perturbation with a vasodilator should consistently increase the dynamic perfusion defect volume.

Conclusions

Baseline perfusion defects from AVMs are related to lesion size rather than to feeding arterial pressure. Regional cerebral hypotension induced by AVMs at the cortical level does not necessarily result in loss of autoregulatory function in adjacent territories. Although cerebral AVMs induce local and distant perfusion changes, attention should be focused on mechanisms that involve mass-related or neurogenic factors rather than exclusive hemodynamic considerations.

References

1. Kumar AJ, Fox AJ, Vinuela F, Rosenbaum AE. Revisited old and new CT findings in unruptured larger arteriovenous malformations of the brain. *J Comput Assist Tomogr* 1984;8:648–655
2. Duncan R. Epilepsy, cerebral blood flow, and cerebral metabolic rate. *Cerebrovasc Brain Metab Rev* 1992;4:105–121
3. Feeney DM, Baron J-C. Diaschisis. *Stroke* 1986;17:817–830
4. Spetzler RF, Wilson CB, Weinstein P, Mehdorn M, Townsend J, Telles D. Normal perfusion pressure breakthrough theory. *Clin Neurosurg* 1978;25:651–672
5. Batjer HH, Devous MD Sr, Meyer YJ, Purdy PD, Samson DS. Cerebrovascular hemodynamics in arteriovenous malformation complicated by normal perfusion pressure breakthrough. *Neurosurgery* 1988;22:503–509
6. Nornes H, Grip A. Hemodynamic aspects of cerebral arteriovenous malformations. *J Neurosurg* 1980;53:456–464

7. Young WL, Pile-Spellman J, Prohovnik I, Kader A, Stein BM, Columbia University AVM Study Project. Evidence for adaptive autoregulatory displacement in hypotensive cortical territories adjacent to arteriovenous malformations. *Neurosurgery* 1994;34:601–611

8. Sullivan HG, Kingsbury TB 4th, Morgan ME, et al. The rCBF response to Diamox in normal subjects and cerebrovascular disease patients. *J Neurosurg* 1987;67:525–534

9. Yonas H, Smith HA, Durham SR, Pentheny SL, Johnson DW. Increased stroke risk predicted by compromised cerebral blood flow reactivity. *J Neurosurg* 1993;79:483–489

10. Young WL, Kader A, Prohovnik I, et al. Pressure autoregulation is intact after arteriovenous malformation resection. *Neurosurgery* 1993;32:491–497

11. Pasqualin A, Barone G, Cioffi F, Rosta L, Scienza R, Pian RD. The relevance of anatomic and hemodynamic factors to a classification of cerebral arteriovenous malformations. *Neurosurgery* 1991;28:370–379

12. Mountz JM. A method of analysis of SPECT blood flow image data for comparison with computed tomography. *Clin Nucl Med* 1989;14:192–196

13. Young WL, Pile-Spellman J. Anesthetic considerations for interventional neuroradiology (Review). *Anesthesiology* 1994;80:427–456

14. Duckwiler G, Dion J, Vinuela F, Jabour B, Martin N, Bentson J. Intravascular microcatheter pressure monitoring: experimental results and early clinical evaluation. *AJNR Am J Neuroradiol* 1990;11:169–175

15. Fleischer LH, Young WL, Pile-Spellman J, et al. Relationship of transcranial Doppler flow velocities and arteriovenous malformation feeding artery pressures. *Stroke* 1993;24:1897–1902

16. Kader A, Young WL, Pile-Spellman J, Columbia University AVM Study Project. The influence of hemodynamic and anatomic factors on hemorrhage from cerebral arteriovenous malformations. *Neurosurgery* 1994;34:801–808

17. Spetzler RF, Hargraves RW, McCormick PW, Zabramski JM, Flom RA, Zimmerman RS. Relationship of perfusion pressure and size to risk of hemorrhage from arteriovenous malformations. *J Neurosurg* 1992;76:918–923

18. Powers WJ. Cerebral hemodynamics in ischemic cerebrovascular disease. *Ann Neurol* 1991;29:231–240

19. Nornes H, Wikeby P. Cerebral arterial blood flow and aneurysm surgery, I: local arterial flow dynamics. *J Neurosurg* 1977;47:810–818

20. Takeuchi S, Kikuchi H, Karasawa J, et al. Cerebral hemodynamics in arteriovenous malformations: evaluation by single-photon emission CT. *AJNR Am J Neuroradiol* 1987;8:193–197

21. Barnett GH, Little JR, Ebrahim ZY, Jones SC, Friel HT. Cerebral circulation during arteriovenous malformation operation. *Neurosurgery* 1987;20:836–842

22. Hassler W, ed. *Hemodynamic Aspects of Cerebral Angiomas*. Vienna, Austria: Springer-Verlag; 1986:136 pages

23. Spetzler RF, Martin NA, Carter LP, Flom RA, Raudzens PA, Wilkinson E. Surgical management of large AVMs by staged embolization and operative excision. *J Neurosurg* 1987;67:17–28

24. Feindel W, Yamamoto YL, Hodge CP. Red cerebral veins and the cerebral steal syndrome: evidence from fluorescein angiography and microregional blood flow by radioisotopes during excision of an angioma. *J Neurosurg* 1971;35:167–179

25. Nagao S, Ueta K, Mino S, et al. Monitoring of cortical blood flow during excision of arteriovenous malformations by thermal diffusion method. *Surg Neurol* 1989;32:137–143

26. Okabe T, Meyer JS, Okayasu H, et al. Xenon-enhanced CT CBF measurements in cerebral AVMs before and after excision: contribution to pathogenesis and treatment. *J Neurosurg* 1983;59:21–31

27. Yamada S, Cojocaru T. Arteriovenous malformations. In: Wood JH, ed. *Cerebral Blood Flow: Physiology and Clinical Aspects*. New York, NY: McGraw-Hill; 1987:580–590

28. Tamaki N, Lin T, Asada M, et al. Modulation of blood flow following excision of a high flow cerebral arteriovenous malformation: case report. *J Neurosurg* 1990;72:509–512

29. Young WL, Prohovnik I, Ornstein E, et al. The effect of arteriovenous malformation resection on cerebrovascular reactivity to carbon dioxide. *Neurosurgery* 1990;27:257–267

30. Hasleton PS, Carr N, Schofield PF. Vascular changes in radiation bowel disease. *Histopathology* 1985;9:517–534

31. Fajardo LF, Berthrong M. Vascular lesions following radiation. *Pathol Annu* 1988;23:297–330

32. Bogsrud TV, Rootwelt K, Russell D, Nyberg-Hansen R. Acetazolamide effect on cerebellar blood flow in crossed cerebral-cerebellar diaschisis. *Stroke* 1990;21:52–55

33. Tanaka K, Yonekawa Y, Kaku Y, Kazekawa K. Arteriovenous malformation and diaschisis. *Acta Neurochir (Wein)* 1993;120:26–32

34. Tyler JL, Leblanc R, Meyer E, et al. Hemodynamic and metabolic effects of cerebral arteriovenous malformations studied by positron emission tomography. *Stroke* 1989;20:890–898

35. Prosenz P, Heiss W-D, Kvicala V, Tschabitscher H. Contribution to the hemodynamics of arterial venous malformations. *Stroke* 1971;2:279–289

36. De Reuck J, Van Aken J, Van Landegem W, Vakaet A. Positron emission tomography studies of changes in cerebral blood flow and oxygen metabolism in arteriovenous malformation of the brain. *Eur Neurol* 1989;29:294–297

37. Fink GR. Effects of cerebral angiomas on perifocal and remote tissue: a multivariate positron emission tomography study. *Stroke* 1992;23:1099–1105

38. Batjer HH, Devous MD Sr, Seibert GB, et al. Intracranial arteriovenous malformation: relationships between clinical and radiographic factors and ipsilateral steal severity. *Neurosurgery* 1988;23:322–328

39. Miyasaka Y, Yada K, Kurata A, Tokiwa K, Tanaka R, Ohwada T. An unruptured arteriovenous malformation with edema. *AJNR Am J Neuroradiol* 1994;15:385–388

40. Berenstein A. Comment on: Sugita M, Takahashi A, Ogawa A, Yoshimoto T. Improvement of cerebral blood flow and clinical symptoms associated with embolization of a large arteriovenous malformation: case report, pp 748–751. *Neurosurgery* 1993;33:752

41. Miyasaka Y, Kurata A, Tokiwa K, Tanaka R, Yada K, Ohwada T. Draining vein pressure increases and hemorrhage in patients with arteriovenous malformation (case report). *Stroke* 1994;25:504–507